Marine and Petroleum Geology 28 (2011) 1634–1647

Contents lists available at ScienceDirect

Marine and Petroleum Geology

journal homepage: www.elsevier.com/locate/marpetgeo

Evaluation of geological factors in characterizing fault connectivity during hydrocarbon migration: Application to the Bohai Bay Basin

Likuan Zhang [a], Xiaorong Luo [a,*], Guy Vasseur [b], Changhua Yu [c], Wan Yang [a,d], Yuhong Lei [a], Chengpeng Song [a], Lan Yu [a], Jianzhao Yan [a]

[a] Key Laboratory of Petroleum Resources Research, Chinese Academy of Sciences, Beijing 100029, China
[b] SISYPHE, UMR7619, Université Pierre et Marie Curie, 75252 Paris Cedex, France
[c] Petroleum Exploration and Development Research Institute of Dagang Oilfield Company Ltd., Tianjin 300280, China
[d] Department of Geological Science & Engineering, Missouri University of Science and Technology, Missouri 65409, USA

ARTICLE INFO

Article history:
Received 23 February 2011
Received in revised form
14 June 2011
Accepted 23 June 2011
Available online 1 July 2011

Keywords:
Fault opening and sealing
Geological parameters
Hydrocarbon migration
Fault-connectivity probability
Bohai Bay basin

ABSTRACT

Faults play an intricate role in hydrocarbon migration and accumulation since they can serve either as a conduit or a seal. Quantitative evaluation of fault opening/sealing properties requires the selection of valid and optimal parameters among numerous geological factors to characterize the hydraulic behaviors of faults. The present study focuses on the Chengbei Step-Fault Area in the Qikou Depression, Bohai Bay Basin, NE China, because hydrocarbon migration and accumulation in this area occurred in a relatively short period so that accumulated hydrocarbons can be used as an indicator to deduce hydraulic connectivity of a fault zone between two sites. Various geological parameters pertinent to a fault, such as burial depth, dip angle, throw, strike, percentage of sandstone of faulted intervals, fluid pressure in faulted mudstone, stress normal to the fault plane, and shale gouge ratio, are analyzed to assess their effectiveness in characterizing fault connectivity. An index, the fault-connectivity probability (N_p), is proposed to evaluate the possibility that a fault has been once serving as a migration pathway. The statistical relationship between N_p and any a geological parameter may be used to indicate the effectiveness of this parameter in characterizing the connectivity of a fault during hydrocarbon migration. The correlation coefficient of a relationship is a good indicator of the effectiveness; and the results are generally in agreement with qualitative assessments. Parameters representing a single geological factor are generally ineffective, whereas those representing implicitly or explicitly two or more factors, such as shale gouge ratio, stress normal to the fault plane, and fault opening index, are more effective.

1. Introduction

Faults play an important role in hydrocarbon migration and accumulation (Smith, 1966, 1980; Berg, 1975; Weber et al., 1978; Galloway et al., 1982; Hooper, 1991; Knipe, 1992; Fisher and Knipe, 1998, 2001), because they can act as conduits or barriers (Sample et al., 1993; Boles and Grivetti, 2000; Eichhubl and Boles, 2000; Boles et al., 2004; Jin et al., 2008) during fluid migration. The dual behavior has been the focus of discussions over several decades (Sibson, 1981, 1994; Losh et al., 1999). Nevertheless, the role of faults in hydrocarbon migration still needs to be better understood.

Previous researchers (Sibson et al., 1975; Hooper, 1991; Moretti, 1998) suggested that local high-permeability segments of a fault serve as flow paths when faulting is active, but as barriers when faulting is inactive. Faulting is a complex process: two walls move relatively in opposite directions and are offset, resulting in some open segments that permit fluid flow (Haney et al., 2005). In fact, a fault plane is generally a zone with complex internal structures, containing possibly subsidiary faults, fractures, fault gouge and breccias, and cataclasites (Chester and Logan, 1986; Smith et al., 1990; Forster and Evans, 1991; Chester et al., 1993; Bruhn et al., 1994; Caine et al., 1996). These internal elements may display different petrophysical and hydraulic properties at different locations and vary with variable geological conditions during basin evolution (Caillet and Batiot, 2003). For example, following a climax tectonic event, the stress which once generated or moved a given fault is probably relaxing so that the fault zone tends to close, and/or the once open zone tends to be gradually cementated (healed) in the ensuing period of quiescence.

The episodic opening and closing of a fault segment can be viewed as a series of complex switches in the history of a basin,

* Corresponding author.
E-mail address: luoxr@mail.igcas.ac.cn (X. Luo).

0264-8172/$ – see front matter © 2011 Elsevier Ltd. All rights reserved.
doi:10.1016/j.marpetgeo.2011.06.008

which characterize the hydraulic behaviors of a fault (e.g., Sibson et al., 1975; Losh et al., 1999; Xie et al., 2001; Jin et al., 2008). The distribution of these switches on a fault plane and fluxes of fluid channeling through the switches, which depend on the aperture of an open fault, are highly variable because geological factors affecting the sealing characteristics of fault zones are numerous and complex (Hasegawa et al., 2005). Specifically, the amount of fluid flow through an open fault segment during each faulting event is variable (Haney et al., 2005)

In most cases, the duration of an active faulting episode is only a fraction of the total life span, of the fault and is even lesser compared to the duration of the entire migration process (Hooper, 1991; Robert and Nann, 1995). As a result, only a small amount of hydrocarbons migrated through a fault segment during one episode of faulting (Haney et al., 2005); and probably thousands upon thousands of faulting episodes and associated migration events are needed to accumulate a commercial quantity of hydrocarbons in a trap (Anderson et al., 1994). The properties of an open fault segment are probably ever-changing and fluid flows during individual migration events behave differently. Fault "opening" and associated hydrocarbon migration are geological processes, representing a series of different physical processes that occurred repeatedly over a geological time span. Any permeability measurements at different localities along a fault zone would only represent the current state of fault sealability, which may differ greatly from that during active faulting and hydrocarbon migration.

Many studies have been devoted to identifying diagnostic parameters that may be universally applied to effective assessing the sealability of faults (e.g., Schowalter, 1979; Watts, 1987; Harding and Tuminas, 1989; Bouvier et al., 1989; Lindsay et al., 1993; Knott, 1993; Yielding et al., 1997; Sorkhabi et al., 2002; Sorkhabi and Tsuji, 2005). Dozens of parameters have been used for evaluating sealability of faults (Bouvier et al., 1989; Lindsay et al., 1993; Knott, 1993; Yielding et al., 1997; Sorkhabi et al., 2002). In fact, any one factor that affects sealability in one or other aspects can be parameterized. However, the effectiveness of a particular parameter varies from case to case (Færseth et al., 2007). The role of a geological factor on fault sealability during hydrocarbon migration must be well understood before the factor can be accurately parameterized and effective.

Zhang et al. (2010) introduced an empirical fault-connectivity probability method to assess the hydraulic connectivity of faults during hydrocarbon migration at a geological time scale. Whether the petroleum migration has already occurred through a fault segment at any point of time in the basin history or not is identified by the presence or absence of hydrocarbon-bearing layers on both sides of the segment. Data from the Chengbei Step-Fault Area (CSFA) in the Qikou Depression, Bohai Bay Basin, northeast China, were used to develop this method. The role of an open fault segment in migration was then assessed by the relationship between the fault-connectivity probability and a parameter called the fault opening index (Zhang et al., 2010).

The hydraulic-connectivity probability concept of Zhang et al. (2010) offers a practically statistical approach to characterize the opening and closing of a fault segment during hydrocarbon migration. Furthermore, it may be used to assess the effectiveness of a parameter that represents the role of one or several geological factors in hydrocarbon migration through a fault. This study is an effort to assess the effectiveness of parameters used in characterizing fault behaviors during hydrocarbon migration, and to compare the effectiveness of various parameters when applied in the CSFA.

2. Parameters characterizing fault connectivity

Many parameters that represent geological factors affecting fault connectivity have been proposed to evaluate whether a fault would have served as a barrier or conduit for hydrocarbon migration (e.g., Harding and Tuminas, 1989; Knott, 1993; Knipe et al., 1997; Sorkhabi et al., 2002; Færseth et al., 2007). Some parameters that can be obtained from routine exploration data are discussed below (Fig. 1):

2.1. Burial depth of a fault segment (Fig. 1a)

The burial depth has a close relationship with fault sealability (e.g., Knott, 1993; Gibson, 1994; Hesthammer et al., 2002; Sperrevik et al., 2002; Yielding, 2002; Bretan et al., 2003). Increasing burial depth implies increasing mechanical compaction and confining pressure, which reduces the porosity and permeability of rocks in the fault zone. Moreover, greater burial depth also implies, in many cases, greater duration of diagenesis, which may promote cementation/healing of open fractures. As a result, the hydraulic connectivity of a fault zone is likely reduced progressively with burial depth (Aydin and Johnson, 1983; Knott, 1993). Therefore, a shallow fault may have a greater connectivity probability than a deep fault.

2.2. Dip angle of a fault plane (Fig. 1b)

The normal stress on the fault plane caused by overburden depends on the dip angle of the fault plane. The steeper a fault plane is, the smaller the stress is. Fractures in a fault zone tend to be open and serve as migration pathways when the normal stress is small. The dip angle of a fault can change significantly due to changes in lithology and petrophysical properties of rocks in the fault zone as a function of burial depth. In general, the dip angle decreases with increasing depth (Jaeger and Cook, 1979), so that faults tend to be closed at depth.

2.3. Throw (vertical displacement) of a fault (Fig. 1c)

Outcrop observations indicate that the width of a fault zone correlates approximately linearly with the amount of throw along a fault (e.g., Robertson, 1983; Hull, 1988; Evans, 1990; Knott, 1993; Childs et al., 1997). Fault throw and connectivity for fluid migration are closely related, but it may probably do not contain linearity. A large fault throw may correlate with a wide fault zone where long, wide, and well-connected fractures and thin fault gouge zones tend to develop due to intense and/or prolonged fault movement. These fractures would tend to form hydraulic pathways (Barton et al., 1995). Intense faulting may, however, cause strong cataclasis of rocks within a fault zone, producing fine materials with a low permeability to reduce hydraulic conductivity (Weber et al., 1978; Lindsay et al., 1993; Fulljames et al., 1997; Weber et al., 1978; Sperrevik et al., 2002).

2.4. Strike of a fault plane (Fig. 1d)

The directions of maximum and minimum horizontal principal stresses relative to the strike of a fault affect the sealability of the fault zone (Linjordet and Skarpnes, 1992) and, thus, fault connectivity. For example, a statistical analysis of strikes of sealing and non-sealing faults in the northern North Sea indicates that zones of low sealability coincide with the direction of the regional maximum horizontal principal stress (Knott, 1993; Harper and Lundin, 1997). In this direction, the normal stress applied to the fault plane is the smallest and, as a result, most fractures within the fault zone are open and conducive to hydrocarbon migration. Faults in an area may have different strikes; and a single fault may have varying strikes at different locations because of variation of stress fields and conjugate shearing. Thus, the strike of a fault plane can be indicative of fault connectivity.

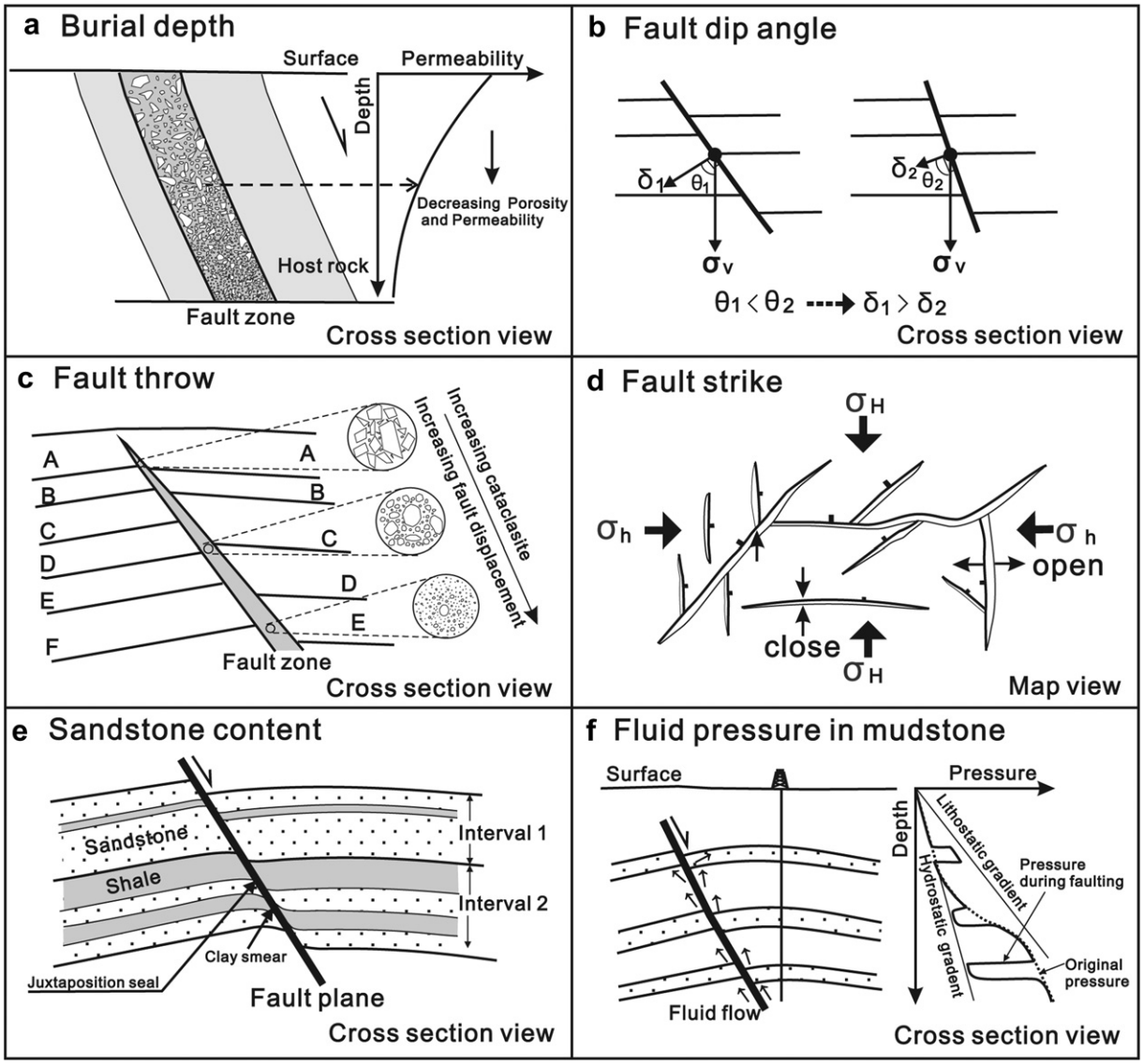

Figure 1. Schematic illustrations showing possible effects of some geologic factors on fault connectivity, which can be quantified using routine exploration data to characterize fault connectivity. (a) Burial depth: With increasing burial depth, permeability of a fault zone generally decreases due to greater mechanical compaction and diagenetic reaction (Aydin and Johnson, 1983; Knott, 1993). (b) Fault dip angle: Faults with a smaller dip angle are more likely to seal due to a greater normal stress on the fault plane, which tends to close open fractures. Where δ is the stress normal to fault plane, θ the fault dip angle and σ_v the vertical stress. (c) Fault throw: A large fault throw correlates with a wide fault zone (e.g., Robertson, 1983) to generate abundant fractures as flow pathways. However, intense faulting may create strong cataclasis of rocks within the fault zone and great reduction in porosity and permeability (Evans, 1990). (d) Fault strike: Most fractures within the fault zone are open in the direction of the regional maximum horizontal principal stress. Fault seal is less likely where there are zones of open factures. Where σ_H and σ_h are respectively maximum and minimum horizontal principal stresses. (e) Sandstone content: Percentage of shale in sandstone-shale successions indicates the potential of clay smear and juxtaposition seal. (f) Fluid pressure in mudstone: During faulting, fluid pressure releases quickly in permeable sandstones, but slowly in shales (e.g., Luo, 1999). High fluid pressure in mudstone indicates a strong tendency of fault opening.

2.5. Sandstone content of a faulted interval (Fig. 1e)

Sandstone content is measured as the thickness percentage of sandstones in a faulted interval composed of sandstone and shale. A small sandstone content, which indicates a large shale content, implies the likelihood of ductile smearing and/or injection of shale within a fault zone (Bouvier et al., 1989; Lindsay et al., 1993; Lehner and Pilaar, 1997; Yielding et al., 1997). In addition, the sandstone content is indicative of the likelihood for sandstone–sandstone juxtaposition across a fault zone (Knott, 1993). The degree of shale smearing and injection and the likelihood of sandstone–sandstone juxtapositon can both affect fault connectivity and, thus, can be used as indicators of fault connectivity.

2.6. Fluid pressure within mudstone (Fig. 1f)

Faulting is a brittle deformation of sedimentary rocks and is closely linked to the mechanical strength of the rocks. The strength is decreasing with increasing abnormal fluid pressure within the strata (Hubbert and Rubey, 1959; Jaeger and Cook, 1979). On the other hand, the release of abnormal overpressure increases the strength. The basic process coupling faulting and fluid pressure changes as follows: fluid pressure build-up, reduction of effective stress and mechanical strength of rocks, rock fracturing, fluid migration, decrease of fluid pressure and increase of rock strength. However, the short time span of fault opening permits significant pressure release only in permeable sandstones, not in shales (Luo,

1999; Luo et al., 2000, 2003). Thus, if hydrocarbon migration and accumulation occurred recently through open faults, the current pressure in mudstones should be an indicator of fault connectivity. That is, a large pressure in mudstone in comparison to that in adjacent sandstone would indicate a strong tendency of fault opening and vice versa.

The aforementioned parameters and understandings on their linkage to geological processes and mechanisms affecting fault connectivity form the basis in our study of fault connectivity in the CSFA, as described below.

3. Parameterization of geological factors controlling fault connectivity

In this paper, data from the CSFA are used to establish a method to assess this effect.

3.1. Geological background of Chengbei Step-Fault area

The Chengbei Step-Fault Area (CSFA) is located on the slope between the Qikou Depression and the Chengning Uplift in the Bohai Bay Basin, NE China, covering an area of ~550 km^2 (Fig. 2a,b). Petroleum exploration in the CSFA began in 1956. During the last five decades, 11 oil-gas fields have been discovered; and proven oil reserves reach 120 million tons. These oil fields are mainly distributed along major faults, suggesting that hydrocarbon migration and accumulation are closely related to fault activity (Fig. 2b).

The structural sketch of the study area consists of a gentle slope cut by multiple step-like faults (Fig. 2a, Wang et al., 2003). There are two major tectonic phases in the study area: a Paleogene syn-rift phase and a Neogene to Quaternary post-rift phase (Li et al., 1998). The Cenozoic strata are composed of continental clastic deposits, with a total thickness of 2000–5000 m. The Paleogene deposits include the Shahejie and Dongying formations (Fig. 2c); the former contains lacustrine and fan delta deposits and the latter contains lacustrine and deltaic deposits. The Neogene to Quaternary succession consists of fluvial deposits of the Guantao, Minghuazhen, and Pingyuan formations (Fig. 2c). A regional rifting-drifting unconformity separates the Paleogene and Neogene strata (Yuan et al., 2004).

The study area has experienced regional transtension since late Mesozoic (Li et al., 1998), resulting in extensive faulting. Major faults are QD, ZDH4, ZB, YEZ, YEZN, and ZHB faults (Yuan et al., 2004; Yu et al., 2006; Fig. 2b). Seismic interpretation indicates that they are syn-sedimentary faults with multi-episodic activities. Zhang et al. (2007) identified three major episodes of intensive faulting during the deposition of Shahejie, Dongying, and upper Minghuazhen formations, respectively.

Hydrocarbons in the CSFA mainly accumulated in the thin sandstones in Sha-3, Sha-2 and Sha-1 members of Shahejie Formation, Guantao Formation, and Ming-2 Member (Fig. 2c). Dark-colored mudstones of Sha-3 and Sha-1 members in the Qikou Depression are the source rocks, and the strata above have no hydrocarbon-generating potential (Wang et al., 2006). Thus, faults are key conduits to vertical hydrocarbon migration into reservoirs of variable ages (Yu et al., 2006; Wang et al., 2006); and multiple oil-bearing reservoirs are vertically stacked and have frequently different hydrocarbon-water contacts (Fig. 2d).

Basin modeling studies of Yu et al. (2006) and Wang et al. (2006) indicate that hydrocarbons were expelled from source rocks during two major episodes. The first episode was at the end of Dongying time (~26 Ma) when source rocks in the Sha-3 Member became mature. Hydrocarbon expulsion ceased because of regional uplifting and erosion at the end of Paleogene. Therefore this early episode of hydrocarbon expulsion is short and the amount of expelled hydrocarbon is limited. Major expulsion occurred during the second episode from late Miocene to Quaternary (Wang et al., 2006). The deposition of the Neogene Guantao and Minghuazhen formations caused maturation and hydrocarbon generation in the Sha-3 and Sha-1 source rocks. Hydrocarbon expulsion peaked at the end of Minghuazhen time (~2 Ma). And the studied area has kept subsiding from then without significant changes in tectonics (Wang et al ., 2003). Thus, the CSFA is particularly suitable for using hydrocarbons as an indicator of fault opening and closing, since hydrocarbons in the CSFA may be considered to be accumulated during the period from Miocene to Pliocene (Yu et al., 2006).

In addition, more than 140 exploratory wells have been drilled, providing a large quantity of well and production data. The entire CSFA area has been covered by 3-D seismic survey, which has been interpreted at a grid resolution of 25 × 25 m for main structural layers. The abundant exploration data greatly facilitate acquisition of various geological parameters to aid in our study of fault connectivity.

3.2. Identification of the opening and closing states of faults during migration

Fluid movement in sedimentary rocks and faults inevitably leaves some evidence, such as diagenetic minerals and fluid inclusions, which can be used as indicators to identify the opening and closing states of a fault during fluid flow (Sorkhabi and Tsuji, 2005). However, the indicators are commonly scattered in rocks and veins associated with fault zones. It is likely to observe these indicators on outcrops, but very difficult in deeply-buried rocks because it is impossible to collect enough cores to study fluid circulation associated with a fault. Finally, multi-episodic circulations of formation waters around fault zones during the entire basin history, which have been previously used as indicators, are too complex to be sorted out accurately.

On the other hand, hydrocarbon generation and migration occur in relatively short time spans. The occurrence of hydrocarbon in two sites, where the source is clear and the driving force for migration is identified, strongly suggests a hydraulic connection between the sites in the past. Hence, the discovered hydrocarbon accumulations can be used as indicators that a fault segment has been open during hydrocarbon migration. In the CSFA, the presence or absence of hydrocarbon accumulations in reservoirs located in both the footwall and hanging-wall of a fault is considered as the indicator of fault opening or closing during the main episode of hydrocarbon migration from late Neocene to early Pliocene (Zhang et al., 2010).

In this study, following the procedures of Zhang et al. (2010), a fault plane is divided into a grid system consisting of intersection lines between stratal surfaces and a fault plane and between the fault plane and seismic sections perpendicular to the fault plane. The grid size depends on 1) the stratigraphic subdivision of studied intervals, 2) density of seismic sections near the fault, and 3) distribution of boreholes. On a seismic section perpendicular to the fault plane, intersecting points between stratal boundaries and the fault plane are taken as identification grid nodes (Fig. 3).

Second, assuming that a fault is the only migration pathway and hydrocarbon migrated upward along the fault plane, whether a node was open or closed during migration is determined by the presence or absence of hydrocarbons in reservoirs above the node on both sides of the fault. For example, nodes A, B, and C on an intersection line on the fault plane have four possible scenarios (Fig. 3b–e) and can be used to identify whether Node B had been open for migration: 1) reservoirs below B contain hydrocarbon and those above do not; 2) both reservoirs above and below B contain

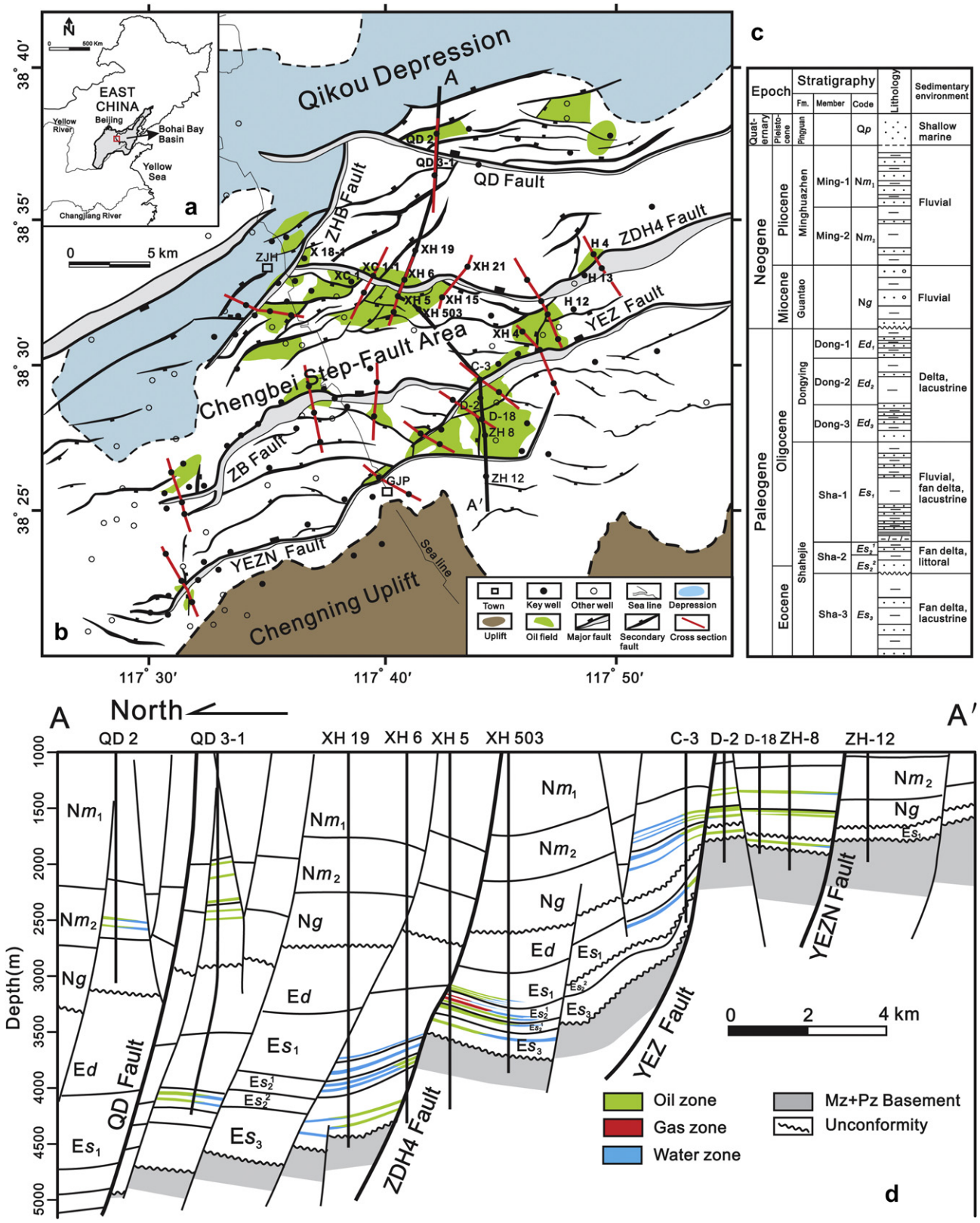

Figure 2. (a) Location of Bohai Bay Basin and the study area (red square) in NE China. (b) Structural map of the Chengbei step-fault area showing faults on top of the Shahejie Formation, oil fields (green area), key wells used in this study (black dots), other wells (black circles), and location of cross sections discussed in the text (red lines). (c) Stratigraphy of the study area, after Yuan et al. (2004). (d) Structural cross section illustrating the stratigraphy, faults, and discovered hydrocarbon zones. See (a) for location.

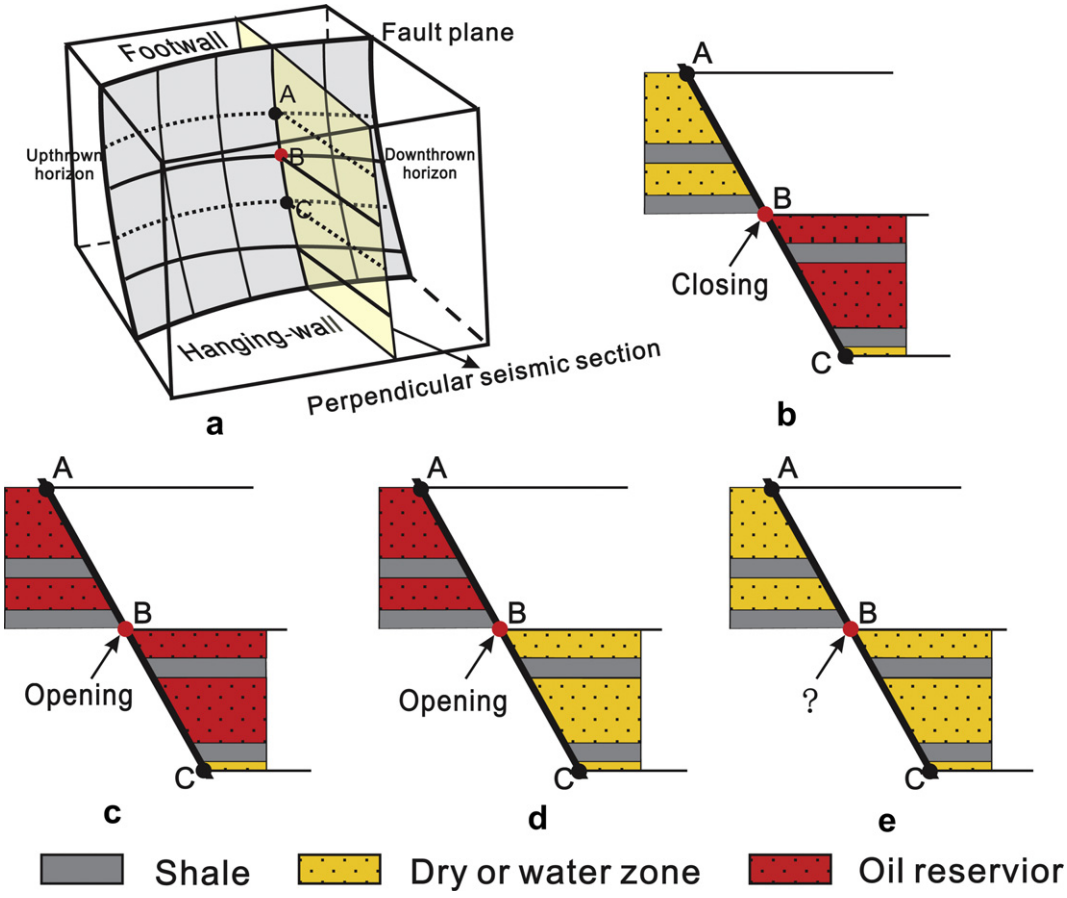

Figure 3. Diagram showing the construction of a grid system on a fault plane and the determination of fault connectivity at a node for hydrocarbon migration. (a) Gridding a fault plane by intersection lines among a fault plane, stratal surfaces, and a seismic section perpendicular to the fault plane. (b)–(e) Possible scenarios of presence and absence of hydrocarbons above and below Node B, which can be used to identify whether B was open or closed for hydrocarbon migration.

hydrocarbon; 3) reservoirs above B contain hydrocarbon and those below do not; and 4) both reservoirs above and below B do not contain hydrocarbon.

It can be inferred that Node B must have been hydraulically open in scenarios 2 and 3 to connect reservoirs above and below the node during migration. In these cases, B is called a connecting node. In contrast, Scenario 1 indicates that hydrocarbon did not migrate upward through Node B and, thus, B was probably closed during migration. In this case, B is called a non-connecting node. Scenario 4 does not provide sufficient information to assess whether Node B was open or closed during hydrocarbon migration. The above method is empirical in determining whether a point on a fault plane was open or closed during migration (Zhang et al., 2010). The method is, however, imperfect, because it simplifies the intricate migration processes within and along a fault zone. It implies, for example, that hydrocarbon migration occurred on a 2-D section, while actual migration took place in a 3-D space and lateral migration might also have occurred within the fault zone.

3.3. Parameter selection

A geological factor controlling fault connectivity does not act alone and is commonly related to other factors. Thus, a parameter selected to assess fault connectivity most likely represents the effect of a group of geological factors, instead of only one factor. In this study, only parameters that can be measured or derived from routine exploration and production data are taken into account.

Sixteen seismic sections from a 3-D seismic volume perpendicular to six major faults are selected, covering 11 oil fields in the CSFA and intersecting 40 wells (Fig. 2a). The spacing among the sections varies, depending on the exploration level of the studied area. The intersection points (i.e. grid nodes) between a fault plane and the surfaces of reservoirs/carrier beds on a seismic section form a grid on the fault plane. The nodes are coded on the basis of presence or absence of hydrocarbons in reservoirs, which is interpreted from drill stem test (DST) data. The code is a binary index termed as fault-connection index (N_f), which is defined as 0 for absence of evidence for migration and 1 for presence. Nodes where the absence or presence cannot be determined are not coded and discarded. Next, values of burial depth, fault dip angle, fault throw, fault strike, sandstone content and mudstone pressure are aquired and assigned to each node. The values are also used to calculate composite parameters, such as shale gouge ratio (SGR) (Yielding et al., 1997), stress normal to the fault plane and fault opening index (Zhang et al., 2010). A set of all these values of parameters are compiled for a total of 117 effective nodes where the presence or absence of hydrocarbon migration can be ascertained.

Finally, the throw of a fault is accounted for: along a cross section, a stratigraphic surface has two intersection points with the fault plane, one on the upthrown side, the other on downthrown side. Eight formations with eight surfaces are taken into account: bases of Upper and Lower Minghuazhen Formation (Nm_1, Nm_2), Guantao Formation (Ng), Dongying Formation (Ed), Sha-1 Member (Es_1), Upper Sha-2 Member (Es_2^1), Lower Sha-2 Member (Es_2^2), and Sha-3 Member (Es_3) (Fig. 2c,d). Thus, the total number of grid nodes along an intersection line is usually 16 on most sections (e.g., Fig. 4).

Values of many parameters (burial depth, fault dip angle, fault throw, fault strike, sandstone content) at a node are obtained

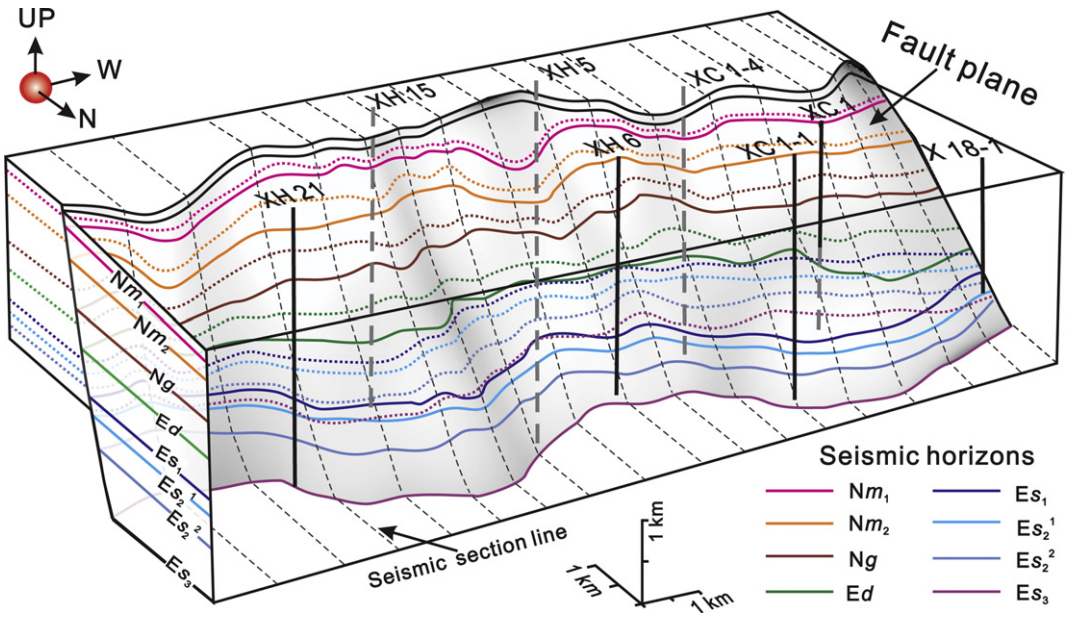

Figure 4. Structural block diagram showing the gridding of Fault ZDH4. The boundaries of stratigraphic intervals are marked as solid lines on the footwall and as dashed lines on the hanging-wall. Vertical lines are wellbores, solid where in front of the fault plane and dashed where behind the fault plane. See Figure 2b for location of the fault and wells.

relatively easily from interpreted seismic sections and wireline logs, structural contour maps, and sandstone content maps. Fluid pressure in mudstone adjacent to the fault plane may be estimated from acoustic logs (Magara, 1978). However these estimates are only available for a limited number of nodes, which is insufficent for this study. Thus, 3-D basin modeling is conducted using the Temis3D software (Ungerer et al., 1990; Schneider et al., 2000), in order to evaluate the fluid pressure at all nodes on all fault planes during the period of hydrocarbon migration. In the model, sediment compaction is assumed to be the main cause of fluid pressure generation. Current fluid pressures are derived from shale compaction curves of 60 wells following the method of Magara (1978). These log-derived pressure data, together with the measured pressure data in DSTs, are used to calibrate the pressure model.

4. Effectiveness of parameters in assessing fault connectivity

Hydrocarbon migration through a fault occurred within the entire fault zone, which can be viewed as a distinct geologic entity, during a geological period and are controlled by a suite of complex geological processes. The concept of fault-connectivity probability is therefore introduced to characterize the composite effect of geological processes in fault-related hydrocarbon migration (Zhang et al., 2010).

4.1. Fault-connectivity probability

It is impossible to determine the hydraulic connectivity for hydrocarbon migration at every node on a fault plane, even in mature exploration areas. However, a statistical treatment of available data points may be used to characterize the hydraulic connectivity of faults as a whole. Fault-connectivity probability serves as a parameter that links fault connectivity with some controlling parameters.

Fault-connectivity probability (N_p) for hydrocarbon migration is defined as the ratio of the number of hydraulically connected nodes (n) to the total number of effective nodes (N):

$$N_p = n/N \quad (1)$$

Commonly the range of values of a parameter at all effective nodes on all fault planes is subdivided into several intervals (e.g., the parameter of burial depth in Fig. 5a). In each interval, the value of N_p is calculated from (1) and plotted at the mid-point of the interval over the entire range of the parameter to illustrate the variability of N_p as a function of the corresponding parameter (Fig. 5b).

The trend of variability shows the effectiveness of a parameter in characterizing the hydraulic connectivity of all the faults used in the statistic analysis. For example, the relationship between burial depth and N_p (Fig. 5b) demonstrates that the fault connectivity tends to decrease with burial depth. The underlying mechanisms for this trend are that shallow burial exerts a relatively small normal stress on a fault plane; and that diagenesis within a fault zone at a shallow depth is commonly weak, resulting in limited healing/cementation in the fractures. As a result, at shallow burial depth, faults are likely hydraulically open with respect to migration.

Furthermore, the effectiveness of a parameter in characterizing fault connectivity for hydrocarbon migration can also be assessed quantitatively using such relationship. Again, using burial depth as an example, it correlates well with N_p in the interval of 1500–3300 m, but not in intervals shallower and deeper. The correlation between burial depth and N_p resulted in a coefficient of determination (R^2) of 0.93 through quadratic regression (dashed regression line in Fig. 5b), which implies that burial depth is a significant parameter for fault connectivity within this interval. The reason is that burial depth represents the effects of many geological factors and processes, such as formation temperature, pressure, conditions for hydrocarbon generation and migration, compaction and diagenesis, and so on. However, these factors and processes may not vary linearly with depth so that burial depth is not a perfect parameter for all depths. For sediments buried shallower than 1500 m, some other factors, such as poor sealability of caprocks or poor migration conditions, may be more influential than depth. For sediment buried deeper than 3300 m, high overpressure may facilitate fracturing and, thus, enhance fault connectivity.

The validity of the relationship between a parameter and N_p is artificially influenced by the subdivision of the range of values of

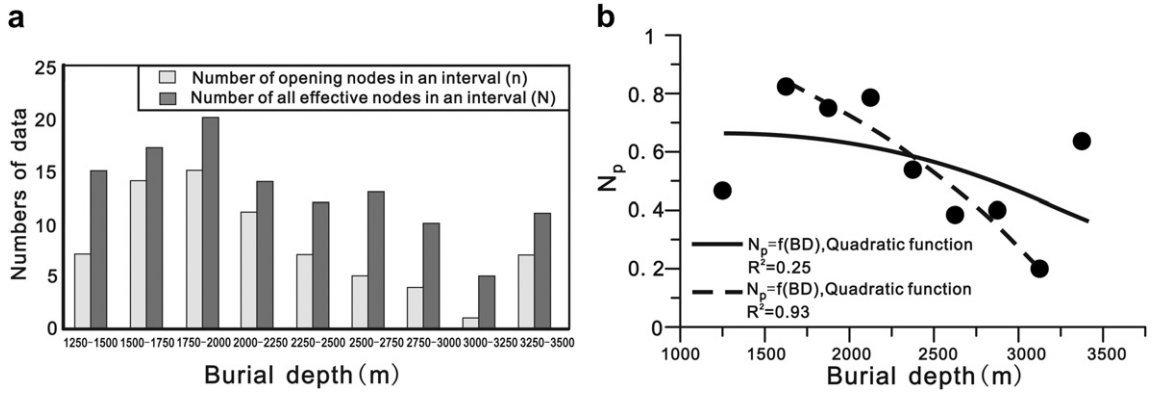

Figure 5. (a) Histogram of the number of opening nodes and the number of all effective nodes on all fault planes in the study area tabulated for individual intervals of buried depth, as an example of subdividing the value range of a parameter and calculating fault-connectivity probability (N_p) of each interval. (b) Relationship between N_p and burial depth (BD). The value of N_p in each interval is plotted at the mid-point of the interval. A statistical relationship is established through regression. The solid regression line is obtained using all data points, whereas the dashed line without using two end points. See text for discussion.

the parameter. If the width of the interval is too large, the number of intervals is limited and the regression relationship is not very significative. On the contrary, narrow intervals may limit the number of data points within some intervals and the N_p values of those intervals is not statistically representative and the observed trend is very scattered. Our empirical rules for optimal subdivision schemes are: 1) the width of the interval should be as small as possible, as long as the number of data points within an interval is statistically reasonable (i.e. $n > 5$); and 2) the correlation coefficient of a relationship established through regression is the the largest among all possible subdivision schemes. These rules are demonstrated using examples of burial depth (Fig. 6). If the interval is small (100 m), the number of data points in some intervals is too small (Fig. 6a), whereas the number of data points is adequate for large intervals of 200, 300, and 400 m (Fig. 6b, c, d). However, in all these cases, the correlation coefficients are much smaller than that of the case in Fig. 5b, where the interval width is 250 m. The correlation coefficient of 0.25 is the largest among many subdivision schemes.

The dependance on interval width in establishing the relationship between a parameter and N_p emphasizes the arbitariness of this approach in assessing the effectiveness of this parameter in characterizing fault connectivity for migration. Some reference is needed to justify this arbitrariness. If a given parameter is perfectly effective, its relationship with N_p should be a step function (curve A in Fig. 7): when the value of the parameter is smaller than a threshold value, N_p is close to zero, indicating a closed fault; and when the value is larger than the threshhold value, N_p is much greater than zero, indicating an open fault during migration. A parameter is completely ineffective if its relationship with N_p is constant (curve B in Fig. 7), that is, variation in the value of the parameter does not affect N_p. In actual situations, the effect of various geological factors controlling fault connectivity cannot be represented by a single parameter. Thus, the relationship of an effective but imperfect parameter with N_p should look like the curve C, or better, like the Curve D in Figure 7.

4.2. Effectiveness of selected parameters in assessing fault connectivity

To evaluate the effectiveness of some parameters in assessing fault connectivity, various parameters, that can be obtained directly or derived from routine exploration and production data, are examined by establishing the relationship between one of the parameters and corresponding fault-connectivity probability (N_p). These parameters include: burial depth, fault dip angle, sandstone content, fault throw, fault strike and fluid pressure in mudstone.

4.2.1. Burial depth

Burial depth values observed at 117 nodes range from 1000 m to 4000 m. The range is subdivided into nine intervals with a spacing of 250 m (Fig. 5a). Although a quadratic relationship between the burial depth and N_p is quite possible, the fitting trend is still poor with a low correlation coefficient of 0.25. However, the overall trend that fault-connectivity probability decreases with increasing depth is consistent with qualitative empirical geological interpretation. Note that if the first point located at the 1500 m interval and the last one located at the 3300 m interval are discarded in the regression, the correlation coefficient increases significantly to 0.93 and the fitting curve becomes much more consistent with what is expected. The implications of burial depth-N_p relationship have been discussed in the aforementioned section.

4.2.2. Fault dip angle

Most faults in the CSFA are listric with dip angle progressively decreasing with the depth. The dip angle data range (25–65°) is divided into eight intervals with an increment of 5° (Fig. 8a). Overall, N_p increases with increasing dip angle. A quadratic relationship with a correlation coefficient of 0.56 is obtained. However, large N_p values (>40%) occur at most intervals, indicating that other geological factors may complicate the effect of dip angle on fault connectivity.

4.2.3. Sandstone content

Sandstone percentage values range from 0 to 80% in the study area. This range is divided into eight intervals with an increment of 10%. A weak quadratic relationship between sandstone content and N_p is obtained with a correlation coefficient of 0.43 (Fig. 8b). Generally, the fault connectivity increases with sandstone content, in agreement with the geological interpretation of Knott (1993).

4.2.4. Fault throw

Faults in this study are major faults in the CSFA and, thus, have large throws greater than 100 m. Nine intervals are divided with an increment of 100 m. A positive quadratic correlation appears between fault throw and N_p, albeit statistically weak, as indicated by a correlation coefficient of 0.05 (Fig. 8c). N_p has large values (>40%) in most intervals (Fig. 8c), similar to that for fault dip angle (Fig. 8a). Thus, fault throw is not an effective parameter in assessing fault connectivity.

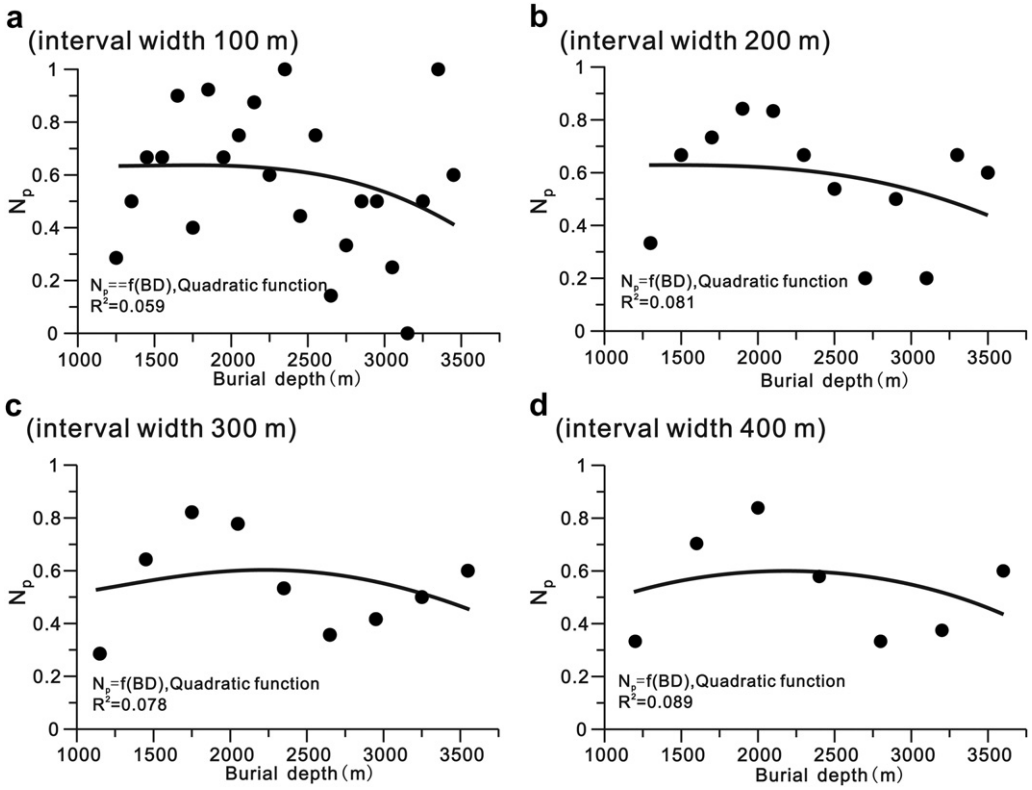

Figure 6. Plots of fault-connectivity probability (N_p) against burial depth (BD), corresponding to four schemes of subdividing the range of values of burial depth, showing the effect of interval width on statistical correlation and the empirical rules for finding the optimal subdivision scheme. See text for discussion.

4.2.5. Fault strike

Fault strike values are divided into ten intervals with an increment of 10°. A moderately strong quadratic correlation between fault strike and N_p is obtained with a correlation coefficient of 0.63 (Fig. 8d). Faults with an orientation between 50 and 100° appear to have a great tendency to be open. The orientation is similar to the direction (55–80°) of regional maximum horizontal principal stress inferred from the borehole collapse data by Qu et al. (1993). Therefore, fault strike and the direction of stress field are effective parameters in assessing fault connectivity in the studied area.

4.2.6. Fluid pressure in mudstone

Fluid pressure values range from 8 to 40 MPa. Seven intervals are used to calculate N_p. A clear quadratic correlation between fluid pressure and N_p is drawn with a correlation coefficient of 0.69 (Fig. 8e). This relationship is supported by qualitative interpretations that a fault zone in highly-overpressured intervals has a better chance to be open.

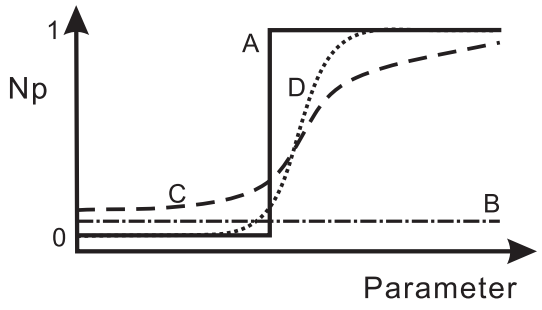

Figure 7. Possible scenarios of the relationship between a parameter and fault-connectivity probability (N_p), as references in determining whether a geological parameter is effective in characterizing fault connectivity for migration. Curve A is the most effective case; Curve B the worst; and Curves C and D the expected ones. See text for discussion.

4.3. Effectiveness of composite parameters in assessing fault connectivity

The above analyses indicate that single geological parameters are not effective in assessing fault connectivity during migration. Composite parameters, that combine two or more single geological parameters associated with hydraulic properties of fault zones (e.g., Bouvier et al., 1989; Lindsay et al., 1993; Yielding et al., 1997), may be more effective in characterizing complex and heterogeneous hydraulic connectivity within fault zones. The effectiveness of some composite parameters is investigated as below.

4.3.1. Shale smear parameters

The shale content in the faulted strata and fault displacement have been speculated as important factors controlling shale smearing (e.g., Weber et al., 1978; Smith, 1980; Lindsay et al., 1993; Yielding et al., 1997). Several parameters considering the two factors have been proposed: Clay Smear Potential (CSP; Bouvier et al., 1989; Fulljames et al., 1997), Shale Smear Factor (SSF; Lindsay et al., 1993), Shale Gouge Ratio (SGR; Fristad et al ., 1997; Yielding et al., 1997), and Smear Gouge Ratio (SMGR; Skerlec, 1996). Among them, the SGR of Yielding et al. (1997) can be used to quickly and accurately estimate the content of shaly material within the fault zone, especially for heterogeneous siliciclastic strata, and is widely used (Sorkhabi and Tsuji, 2005). SGR is defined as the ratio between total thickness of shale in the faulted segment and the fault throw. The shale thickness can be interpreted from gamma-ray logs of wells near the faults.

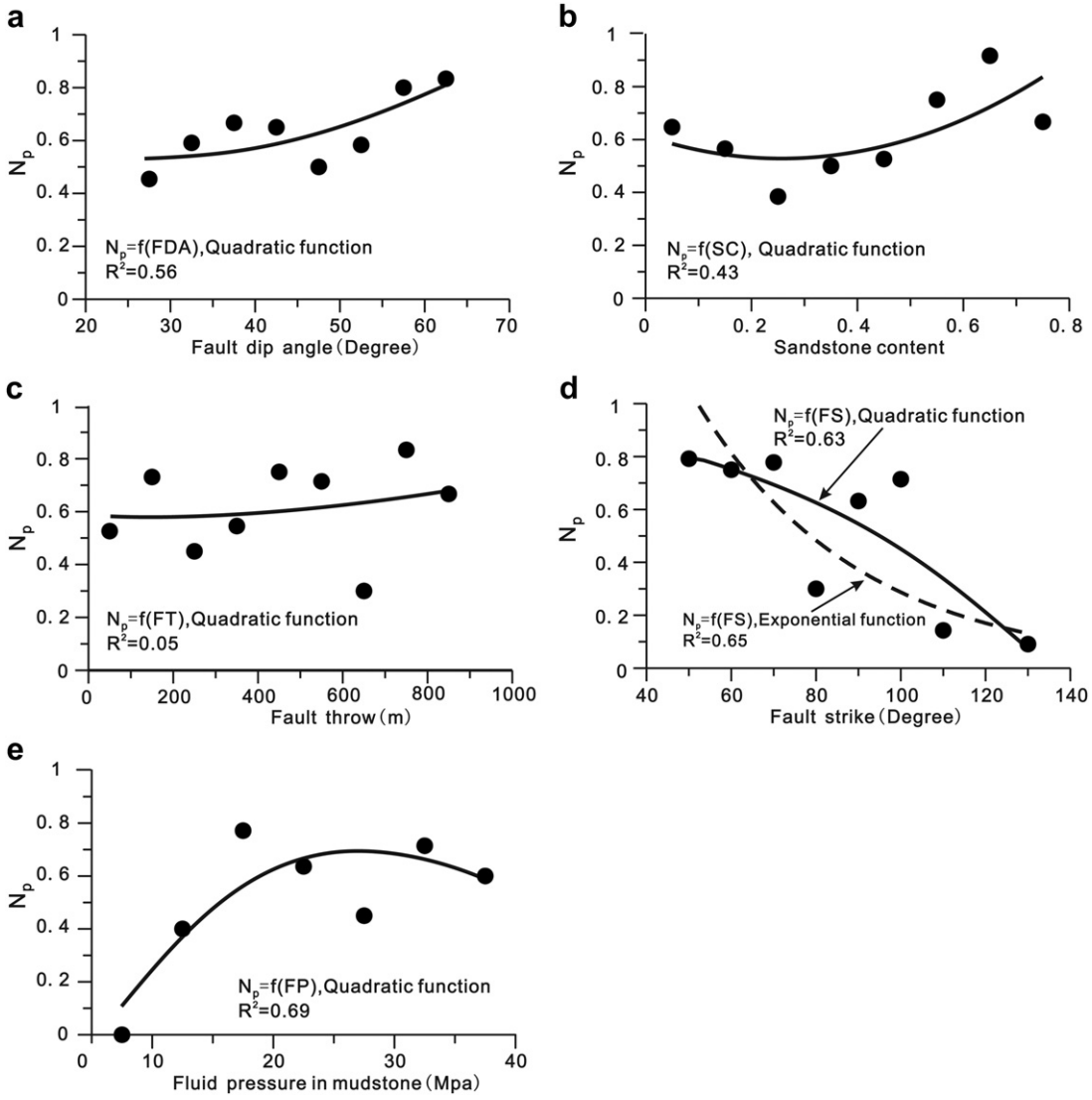

Figure 8. Relationships between fault-connectivity probability N_p and fault dip angle (FDA) (a), sandstone content (SC) (b), fault throw (FT) (c), fault strike (FS) (d), and fluid pressure in mudstone (FP) (e). These weak and moderately strong relationships indicate that single geologic parameters may not be effective in characterizing fault connectivity for hydrocarbon migration. See text for discussions.

117 SGR values are divided into 10 intervals with a 0.1 spacing. The relation between SGR and N_p is similar to the curve D in Figure 7 and the relationship may be expressed as:

$$N_p = \begin{cases} 1 & SGR \le 0.15 \\ f(SGR) & 0.15 < SGR < 0.9 \\ 0 & SGR \ge 0.9 \end{cases} \quad (2)$$

A statistically significant negative quadratic relationship between SGR and N_p with a correlation coefficient of 0.89 is obvious within the interval of SGR value from 0.15 to 0.9 (Fig. 9a). The relationship indicates that a shale smeared fault segment is likely to be closed. The probability of a fault opening as migration pathway is high when SGR value is smaller than 0.45, but is extremely low when SGR value is greater than 0.70.

4.3.2. Stress normal to the fault plane

Several parameters, such as burial depth, dip angle and strike of a fault plane, direction and magnitude of tectonic stress are related to mechanical stresses arising from the overlying strata and tectonic stress field on a fault plane. With respect to fault connectivity, the essential factor represented by these parameters is the effective component stress normal to the fault plane. Large normal stress tends to cause plastic rock deformation during faulting to close fractures (Harding and Tuminas, 1989); otherwise, fractures may stay open and serve as conduits to fluid flow (Zhou et al., 2000; Lu and Ma, 2002). For any stress field, the normal component of the stress acting on a fault plane is (Jaeger and Cook, 1979):

$$\delta = (\sin\alpha \cdot \sin\theta)^2 \sigma_H + (\cos\alpha \cdot \sin\theta)^2 \sigma_h + \cos\theta^2 \sigma_v \quad (3)$$

where δ is the stress normal to the fault plane in MPa; θ is fault dip angle; α is the angle between fault strike and the direction of maximum horizontal principal stress; σ_H, σ_h and σ_v are maximum horizontal principal stress, minimum horizontal principal stress, and vertical stress, respectively. The fault strike, dip angle and burial depth can be obtained as described above. The current stress field in the study area has been studied by Qu et al. (1993) and Xu et al. (1996) using wellbore breakout and hydro-fracturing data

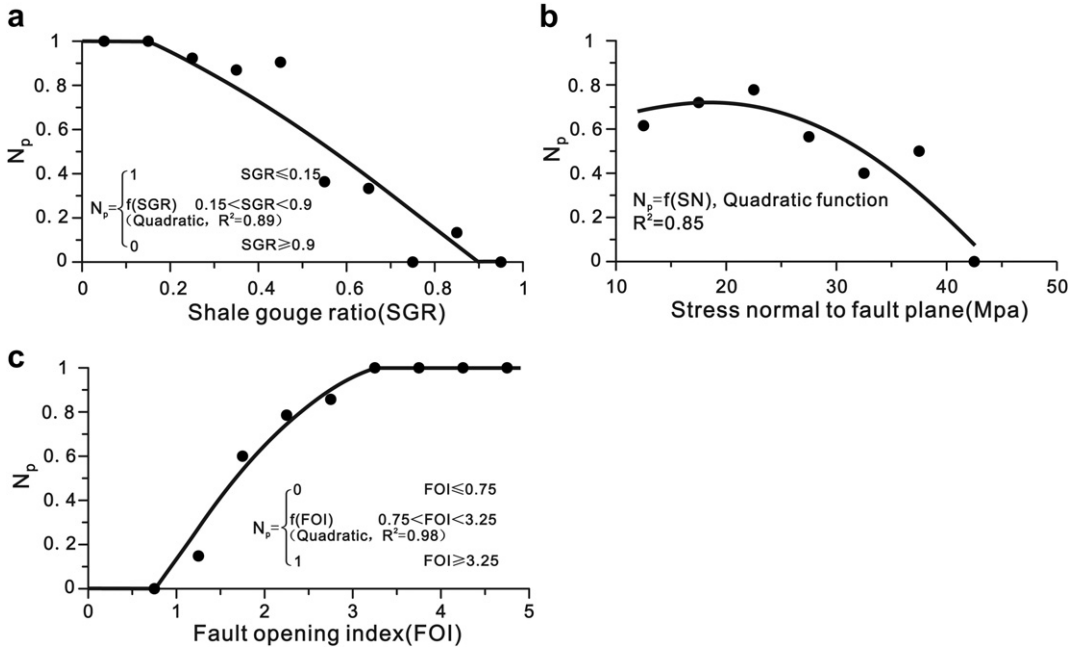

Figure 9. Relationships between fault-connectivity probability N_p and composite parameters of shale gouge ratio (SGR) (a), stress normal to the fault plane (SN) (b), and fault opening index (FOI) (c). The statistically significant relationships indicate that these composite parameters are effective indicators of fault connectivity for hydrocarbon migration.

from about 50 wells. The maximum stress is vertical and the direction of maximum horizontal principal stress is 55–80°. The values of the horizontal principal stresses, σ_H and σ_h, following the burial depth, were estimated from the measurements of Xu et al. (1996).

The values of δ at 117 nodes are divided into eight intervals with an increment of 5 MPa. A dominantly negative quadratic relationship between δ and N_p is evident as indicated by a correlation coefficient of 0.85 (Fig. 9b). Faults are more likely closed when the stress normal to the fault plane is larger. The robustness of this relationship using composite fault-related parameters is much better than any of those using single parameters (including burial depth, fault dip angle, and fault strike) (Fig. 8).

4.3.3. Fault opening index

The strong relationships between N_p and fluid pressure in mudstone, normal stress perpendicular to fault plane, and shale gouge ratio indicate that the three parameters are effective in assessing fault connectivity during migration. They are incorporated into yet another composite parameter, the fault opening index (FOI). It is defined as a dimensionless coefficient (Zhang et al., 2010):

$$\mathrm{FOI} = \frac{P}{\delta \cdot SGR} \tag{4}$$

FOI is the ratio between factors favoring fault opening, represented by the fluid pressure in mudstone(P), and factors promoting fault closure, represented by shale gouge ratio (SGR) and stress normal to the fault plane (δ).

The values of FOI are calculated from the values of the three parameters. They range from 0.5 to 5 and are subdivided into nine intervals with an increment of 0.5. As the relation between FOI and N_p is also similar to the curve D in Figure 7, the relationship may be expressed as following:

$$N_p = \begin{cases} 0 & \mathrm{FOI} \le 0.75 \\ \mathrm{f(FOI)} & 0.75 < \mathrm{FOI} < 3.25 \\ 1 & \mathrm{FOI} \ge 3.25 \end{cases} \tag{5}$$

A well-defined quadratic relationship between FOI and N_p is evident as indicated by a correlation coefficient of 0.98 within the value range from 0.75 to 3.25 (Fig. 9c). This relationship is the best defined among all of those discussed above (Figs. 5, 8, and 9). It suggests that FOI may be the most effective parameter to characterize the hydraulic connectivity of faults for hydrocarbon migration in the studied area. This is because FOI combines parameters to represent the effects of several significant geological factors controlling the hydraulic properties of active faults.

Zhang et al. (2010) demonstrated that in the CSFA N_p is zero when FOI is smaller than 0.75; N_p increases from zero to 1 following a quadratic relationship when FOI changes from 0.75 to 3.25; and N_p is 1 when FOI is larger than 3.25. The values of fault-connectivity probability can be contoured on a fault plane to characterize the variations of hydraulic connectivity of a fault. The applicability of this concept, in particular, the quantitative relationship between FOI and N_p, needs to be tested for other petroliferous basins in the world.

Table 1
Correlation coefficients between geological parameters and N_p determined by regression analysis with different regressive functions.

Parameters	R^2 for different regressive functions				
	Linear	Logarithmic	Inverse	Quadratic	Exponential
Burial depth vs. N_p	0.22	0.18	0.12	0.25	0.23
Fault dip angle vs. N_p	0.52	0.49	0.47	0.55	0.50
Sandstone content vs. N_p	0.28	0.10	0.01	0.43	0.26
Fault throw vs. N_p	0.04	0.03	0.03	0.05	0.01
Fault strike vs. N_p	0.61	0.57	0.52	0.63	0.65
Fluid pressure in mudstone vs. N_p	0.39	0.58	0.71	0.69	0.39
Shale gouge ratio vs. N_p	0.89	0.66	0.33	0.89	0.45
Stress normal to the fault plane vs. N_p	0.66	0.52	0.37	0.85	0.40
Fault opening index vs. N_p	0.80	0.93	0.92	0.98	0.43

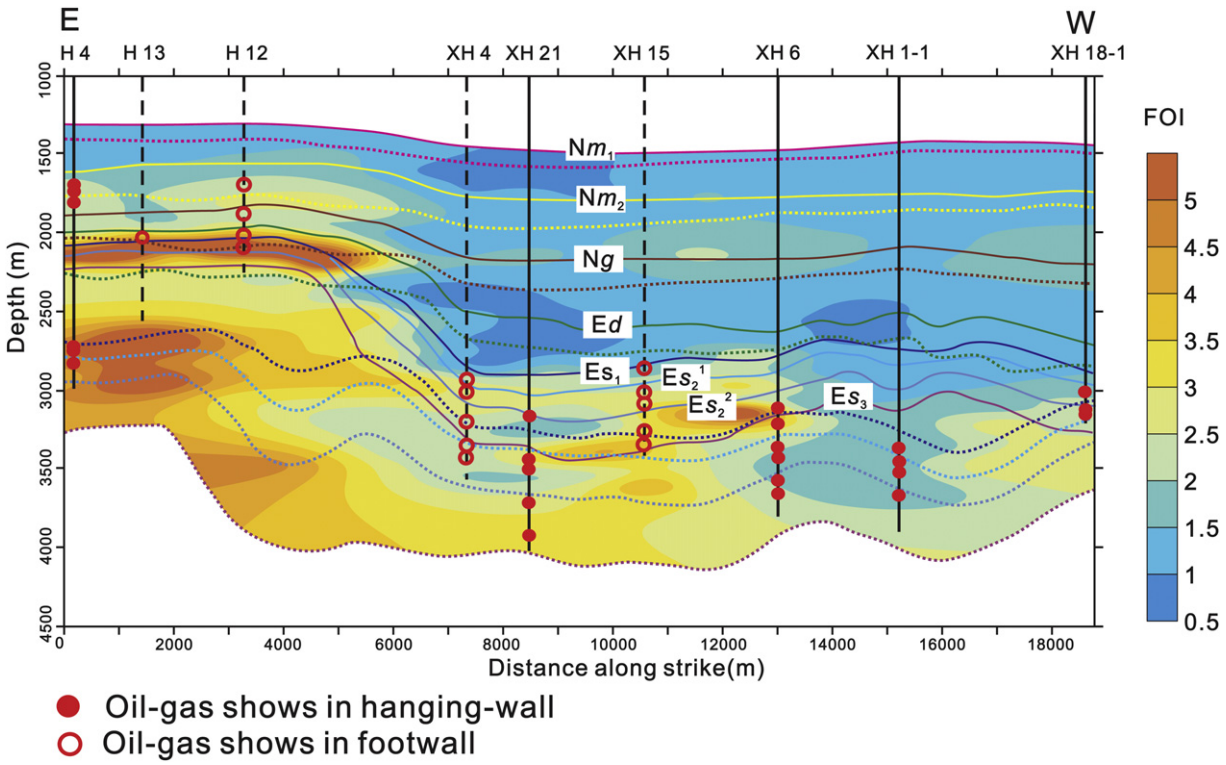

Figure 10. Distribution of FOI on the plane of Fault ZDH4 projected onto a vertical plane. Vertical lines delineate wellbores, solid are in front of the fault plane (on hanging-wall) and dashed are behind the fault plane (on foot-wall). Accumulations discovered in the wells of hanging-wall and footwall are marked by red dots and red circles respectively. Letter-symbols are the codes of strata (Fig. 2). The line styles and annotation of stratigraphic intervals are the same as in Figure 4.

5. Discussions and conclusions

The role of faults in hydrocarbon migration, although generally acknowledged (Smith, 1966, 1980; Berg, 1975; Knipe, 1992; Fisher and Knipe, 1998; Fisher and Knipe, 2001), is rather difficult to be assessed. Considering the multitude of geological factors and processes affecting fault activities and fluid flow, the principal problems lie in the definition of valid parameters to be used to evaluate the controls on fault connectivity during hydrocarbon migration over a long geologic period.

However, the complexity and uncertainty of faulting and associated fluid flow prohibit, in many cases, identification of the major factors or processes affecting hydrocarbon migration. As a result, the validity and effectiveness of a parameter to be used to assess hydraulic fault connectivity during hydrocarbon migration and the applicability of such parameter for different types of fault in different basins are difficult to be determined. For example, the diagenesis in a fault zone is difficult to be quantified and predicted by simple parameter (Knipe, 1992). Actually the fact that the fault sealing efficiency is related to burial depth reflects to a certain extent the influence of diagenesis. When the burial depth exceeds 3000 m, temperature reaches 90 °C and quartz cementation may occur and increase the sealing capacity of a fault zone (Fisher and Knipe, 2001). On another hand, the burial depth is also considered as a factor affecting the stress normal to the fault plane. In addition, fault activity, which may be indicated by fault throw, should also be an important factor to determine the fault connectivity. However, the fault throw is only a crude indicator of cumulated fault activity. Actually the fault activity needs to be analyzed with consideration of the timing of hydrocarbon migration and accumulation.

No single parameter can likely represent all geological factors and processes affecting the fault connectivity during migration, because any parameter that can be acquired from subsurface data reflects only limited aspects of the hydraulic properties of faults particularly in the present geological context (Hesthammer and Fossen, 2000; Yielding, 2002). A possible way of overcoming these difficulties is to introduce some statistic analysis into studies of fault connectivity during migration. Considering the complexity of geofluid flow and their relation with active faults, the use of probability concept on hydraulic fault connectivity seems an effective approach for characterizing fault behaviors during hydrocarbon migration.

This study focuses on hydraulic connectivity (rather than sealability) of faults because hydrocarbon migration may have occurred only during a short episode of active faulting, which caused fracturing to increase hydraulic transmissibility. In contrast, the concept of fault sealing requires only that capillary pressure of a fault plane be evaluated to determine whether hydrocarbons may migrate through the fault or not. Furthermore, it is commonly implied that the sealing state of a fault may be the same over the entire fault plane during hydrocarbon migration. In fact, hydrocarbon fluid flow along fault zones is rather complex, because the permeability of a fault zone is highly heterogeneous and is controlled by many factors. Fluid flow may have occurred in some segments of a fault with a high permeability, while other segments remained impermeable (Sibson, 1981; Moretti, 1998), even though the sealing states of all segments are presently similar.

The relationships between the single and composite parameters and fault-connectivity probability (N_p) demonstrate the varying effectiveness of these parameters in characterizing fault connectivity. In addition, the role of a geologic factor/process on fault

connectivity varies with depth and, thus, a parameter representing a single geologic factor may become less or more effective with depth. On the other hand, composite parameters are more effective for a wide range of depth, because they represent multiple geologic factors and processes (Zhang et al., 2010).

The regression analysis method has been used to establish a fitting relationship between a parameter and a corresponding N_p. To explore a suitable regressive curve for all selected parameters, regressive functions commonly used in Statistical Product and Service Solutions software were tested with the following parameters: burial depth, fault dip angle, sandstone content, fault throw, fault strike, fluid pressure in mudstone, shale gouge ratio, stress normal to the fault plane and fault opening index.

The calculated correlation coefficients between each parameter and the corresponding N_p are listed in Table 1. From Table 1, it can be observed that the correlation coefficient values obtained with the quadratic function are the largest for most parameters, except the fault strike. However, even for this parameter, the value of the quadratic correlation ($R^2 = 0.63$) is similar to the largest one obtained by exponential regression ($R^2 = 0.65$) (Fig. 8d). Therefore, we consider that the correlation coefficient of the quadratic function should be the best measure to establish the fitting relationships.

The distribution of well-characterized fault-connectivity probability on a fault plane is normally predetermined to reconstruct the fault-carrier model for migration simulation (Luo et al., 2007). However, the parameters characterizing the fault sealing or connectivity may also be used to analyze the role of a fault during migration and to provide important information for further exploration. Figure 10 is a vertical section along the ZDH4 fault strike and on which it is illustrated the projection of the distribution of FOI on the ZDH4 fault plane and the presence of discovered hydrocarbon in the hanging-wall and the foot-wall. In this case, hydrocarbons migrated from north along the Shahejie Formation (including members Es_3, Es_2^2, Es_2^1 and Es_1 in Fig. 10) to south and migrated through the fault plane dipping northward. In this case, the distribution of FOI values (corresponding to connectivity) on that fault is heterogeneous (Fig. 10). In general, hydrocarbon accumulations may be found in the fault segments where the FOI values are larger than 1.5, and the depth is deeper than 3000 m in the western area, and at 1500 m depth in the eastern area of the fault plane. The large FOI value segments lie principally towards the east and seem to be controlled by formations. That means that the fault plane at the western part is close during migration in areas shallower than 3000 m. Such FOI value distribution explains why hydrocarbon accumulations have been discovered in Ng and Nm_2 formations at the eastern parts.

The concept of fault-connectivity probability discussed in this study suggests to carry out further statistical analyses on other fault zones that have once, eventually, been used as conduits for large-quantity hydrocarbon migration. The methods developed in this study can evaluate the overall role of the fault zone as a barrier or conduit during the entire process of hydrocarbon migration. Finally, the method can be used to determine the effectiveness of a parameter in assessing fault connectivity during hydrocarbon migration.

Acknowledgment

This study was supported by the Chinese National Natural Science Foundation (40902041) and Chinese National Major Fundamental Research Developing Project (2011CB201105). Qianjin Liao, Shuqin Yuan, and Junqing Su of Dagang Oil Company are acknowledged for providing basic data and helpful discussion. We thank Beicip-Franlab for providing the Temis3D software used in our pressure modeling. We appreciate the comments and encouragement from Y. F. Wang, the reviewers Dr. Leonardo Duerto and Dr. Frederic Schneider, and the editor Alejandro Escalona, who have helped us improving the manuscript.

References

Anderson, R., Flemings, P., Losh, S., Austin, J., Woodhams, R., 1994. Gulf of Mexico growth fault drilled, seen as oil, gas migration pathway. Oil & Gas Journal 92, 97–103.

Aydin, A., Johnson, A.M., 1983. Analysis of faulting in porous sandstones. Journal of Structural Geology 5, 19–31.

Barton, C.A., Zoback, M.D., Moos, D., 1995. Fluid flow along potentially active faults in crystalline rock. Geology 23, 683–686.

Berg, P.R., 1975. Capillary pressure in stratigraphic traps. AAPG Bulletin 59, 939–956.

Boles, J.R., Grivetti, M., 2000. Calcite cementation along the Refugio/Carneros fault, coastal California. A link between deformation, fluid movement and fluid-rock interaction at a basin margin. Journal of Geochemical Exploration 69–70, 313–316.

Boles, J.R., Eichhubl, P., Garven, G., Chen, J., 2004. Evolution of a hydrocarbon migration pathway along basin bounding faults. Evidence from fault cement. AAPG Bulletin 88, 947–970.

Bouvier, J.D., Kaars-Sijpesteijn, C.H., Kluesner, D.F., Onyejekwe, C.C., Van der Pal, R.C., 1989. Three-dimensional seismic interpretation and fault sealing investigations, Nun river field, Nigeria. AAPG Bulletin 73, 1397–1414.

Bretan, P., Yielding, G., Jones, H., 2003. Using calibrated shale gouge ratio to estimate hydrocarbon column heights. AAPG Bulletin 87, 397–413.

Bruhn, R.L., Parry, W.T., Yonkee, W.A., Thompson, T., 1994. Fracturing and hydrothermal alteration in normal fault zones. Pure and Applied Geophysics 142, 609–644.

Caillet, G., Batiot, S., 2003. 2D modeling of hydrocarbon migration along and across growth faults. an example from Nigeria. Petroleum Geoscience 9, 113–124.

Caine, J.S., Evans, J.P., Forster, C.B., 1996. Fault zone architecture and permeability structure. Geology 24, 1025–1028.

Chester, F.M., Logan, J.M., 1986. Implications for mechanical properties of brittle faults from bservations of the Punchbowl fault zone, California. Pure and Applied Geophysics 124, 79–106.

Chester, F.M., Evans, J.P., Biegel, R.L., 1993. Internal structure and weakening mechanisms of the San Andreas fault. Journal of Geophysical Research 98, 771–786.

Childs, C., Walsh, J.J., Watterson, J., 1997. Complexity in fault zone structure and implications for fault seal prediction. In: Møller-Pedersen, P., Koestler, A.G. (Eds.), Hydrocarbon Seals: Importance for Exploration and Production. Norwegian Petroleum Society (NPF), vol. 7. Special Publication, Trondheim, Norway, pp. 61–72.

Eichhubl, P., Boles, J.R., 2000. Rates of fluid flow in fault systems – Evidence for episodic rapid fluid flow in the Miocene Monterey formation, coastal California. American Journal of Science 300, 571–600.

Evans, J.P., 1990. Thickness-displacement relationships for fault zones. Journal of Structural Geology 12, 1061–1065.

Færseth, R.B., Johnsen, E., Sperrevik, S., 2007. Methodology for risking fault seal capacity: implications of fault zone architecture. AAPG Bulletin 91, 1231–1246.

Fisher, Q.J., Knipe, R.J., 1998. Fault sealing processes in siliciclastic sediments. In: Jones, G., Fisher, Q., Knipe, R.J. (Eds.), Faulting, Fault Sealing and Fluid Flow in Hydrocarbon Reservoirs, vol. 148. Geological Society (London), Special Publication, pp. 117–134.

Fisher, Q.J., Knipe, R.J., 2001. The permeability of faults within siliciclastic petroleum reservoirs of the North Sea and Norwegian continental shelf. Marine and Petroleum Geology 18, 1063–1081.

Forster, C.B., Evans, J.P., 1991. Hydrogeology of thrust faults and crystalline thrust sheets. Results of combined field and modeling studies. Geophysical Research Letters 18, 979–982.

Fristad, T., Groth, A., Yielding, G., Freeman, B., 1997. Quantitative fault seal prediction- a case study from Oseberg Syd. In: Møller-Pedersen, P., Koestler, A.G. (Eds.), Hydrocarbon Seals: Importance for Exploration and Production. Norwegian Petroleum Society (NPF), vol. 7. Special Publication, Trondheim, Norway, pp. 107–124.

Fulljames, J.R., Zijerveld, L.J.J., Franssen, R.C.M.W., 1997. Fault seal processes: systematic analysis of fault seals over geological and production time scales. In: Møller-Pedersen, P., Koestler, A.G. (Eds.), Hydrocarbon Seals: Importance for Exploration and Production. Norwegian Petroleum Society (NPF), vol. 7. Special Publication, Trondheim, Norway, pp. 51–59.

Galloway, W., Henry, C., Smith, G., 1982. Depositional Framework, Hydrostratigraphy, and Uranium Mineralization of the Oakville Sandstone (Miocene), Texas coastal plain. University of Texas at Austin, Bureau of Economic Geology Report of Investigations 113, pp. 51.

Gibson, R.G., 1994. Fault-zone seals in siliciclastic strata of the Columbus Basin, offshore Trinidad. AAPG Bulletin 78, 1372–1385.

Haney, M.M., Snieder, R., Sheiman, J., Losh, S., 2005. A moving fluid pulse in a fault zone. Nature 437, 46.

Harding, T.P., Tuminas, A.C., 1989. Structural interpretation of hydrocarbon traps sealed by basement normal blocks and at stable flank of foredeep basins and at rift basins. AAPG Bulletin 73, 812–840.

Harper, T.R., Lundin, E.R., 1997. Fault seal analysis: reducing our dependence on empiricism. In: Møller-Pedersen, P., Koestler, A.G. (Eds.), Hydrocarbon Seals: Importance for Exploration and Production. Norwegian Petroleum Society (NPF), vol. 7. Special Publication, Trondheim, Norway, pp. 149–165.

Hasegawa, S., Sorkhabi, R., Iwanaga, S., Sakuyama, N., Mahmud, O.A., 2005. Fault-seal analysis in the Temana field, offshore Sarawak, Malaysia. In: Sorkhabi, R., Tsuji, Y. (Eds.), Faults, Fluid Flow, and Petroleum Traps. AAPG Memoir, vol. 85, pp. 43–58.

Hesthammer, J., Fossen, H., 2000. Uncertainties associated with fault sealing analysis. Petroleum Geoscience 6, 37–45.

Hesthammer, J., Bjørkum, P.A., Watts, L., 2002. The effect of temperature on sealing capacity of faults in sandstone reservoirs: examples from the Gullfaks and Gullfaks Sør fields, North Sea. AAPG Bulletin 86, 1733–1751.

Hooper, E.C.D., 1991. Fluid migration along growth faults in compacting sediments. Journal of Petroleum Geology 14, 161–180.

Hubbert, M.K., Rubey, W.W., 1959. Role of fluid pressure in mechanics of overthrust faulting. Bulletin of the Geological Society of America 70, 115–205.

Hull, J., 1988. Thickness-displacement relationships for deformation zones. Journal of Structural Geology 10, 431–435.

Jaeger, J.C., Cook, G., 1979. Fundamentals of Rock Mechanics. Chapman and Hall, London, p. 593.

Jin, Z.J., Cao, J., Hu, W.X., Zhang, Y.J., Yao, S.P., Wang, X.L., Zhang, Y.Q., Tang, Y., Shi, X.P., 2008. Episodic petroleum fluid migration in fault zones of the northwestern Junggar Basin (northwest China): evidence from hydrocarbon-bearing zoned calcite cement. AAPG Bulletin 92, 1225–1243.

Knipe, R.J., 1992. Faulting processes and fault seal. In: Larsen, R.M., Brekke, H., Larsen, B.T., Talleraas, E. (Eds.), Structural and Tectonic Modeling and Its Application to Petroleum Geology. Norwegian Petroleum Society(NPF), vol. 1. Special Publication, Stavanger, pp. 325–342.

Knipe, R.J., Fisher, Q.J., Jones, G., Clennell, M.R., Farmer, A.B., Harrison, A., Kidd, B., McAllister, E., Porter, J.R., White, E.A., 1997. Fault seal analysis: successful methodologies, application and future directions. In: Møller-Pedersen, P., Koestler, A.G. (Eds.), Hydrocarbon Seals: Importance for Exploration and Production. Norwegian Petroleum Society (NPF), vol. 7. Special Publication, Trondheim, Norway, pp. 15–40.

Knott, S.D., 1993. Fault seal analysis in the North Sea. AAPG Bulletin 77, 778–792.

Lehner, F., Pilaar, W., 1997. The emplacement of clay smears in syn-sedimentary normal faults. inference from field observations near Frechen, Germany. In: Møller-Pedersen, P., Koestler, A.G. (Eds.), Hydrocarbon Seals: Importance for Exploration and Production. Norwegian Petroleum Society (NPF), vol. 7. Special Publication, Trondheim, Norway, pp. 39–50.

Li, S.T., Lu, F.X., Lin, C.S., 1998. Evolution of Mesozoic and Cenozoic Basins in East China and Their Geodynamic Background (In Chinese). China University of Geosciences Press, Wuhan, p. 238.

Lindsay, N.G., Murphy, F.C., Walsh, J.J., Watterson, J., 1993. Outcrop Studies of Shale Smears on Fault Surfaces. International Association of Sedimentologists, vol. 15. Special Publication. 113–123.

Linjordet, A., Skarpnes, O., 1992. Application of horizontal stress directions interpreted from borehole breakouts recorded by four arm dipmeter tools. In: Vorren, T.O. (Ed.), Arctic Geology and Petroleum Potential. Norwegian Petroleum Society(NPF), vol. 2. Special Publication, pp. 681–690.

Losh, S., Eglington, L., Schoell, P., Wood, J., 1999. Vertical and lateral fluid flow related to a large growth fault, south Eugene Island Block 330, offshore Louisiana. AAPG Bulletin 82, 1694–1710.

Lu, Y.F., Ma, F.J., 2002. Controlling Factors and Classification of Fault Seal (In Chinese), vol. 33. Journal of Jilin University (Earth Science Edition). 163–167.

Luo, X.R., 1999. Mathematical modeling of temperature-pressure transient variation in opening fractures and sedimentary formations (in Chinese). Oil & Gas Geology 20, 1–6.

Luo, X.R., Yang, J.H., Wang, Z.F., 2000. The overpressuring mechanisms in aquifers and pressure prediction in basins (in Chinese). Geological Review 46, 6–10.

Luo, X.R., Dong, W.L., Yang, J.H., Yang, W., 2003. Overpressuring mechanisms in the Yinggehai basin, south China Sea. AAPG Bulletin 87, 629–645.

Luo, X.R., Yu, J., Zhang, L.P., Yang, Y., Chen, R.Y., Chen, Z.K., Zhou, B., 2007. Numerical modeling of secondary migration and its Applications to Chang-8 member of Yanchang formation (Upper Triassic), Longdong area, Ordos basin, China. Science in China Series D: Earth Sciences 50 (Supp. II), 91–102.

Magara, K., 1978. Compaction and Fluid Migration, Practical Petroleum Geology. Elsevier, Amsterdam, p. 319.

Moretti, I., 1998. The role of faults in hydrocarbon migration. Petroleum Geoscience 4, 81–94.

Qu, G.S., Zhang, H., Ye, H., 1993. The principal stress orientations by the borehole breakouts in Huanghua Depression (in Chinese). North China Earthquake Sciences 11, 9–18.

Roberts, S.J., Nunn, J.A., 1995. Episodic fluid expulsion from geopressured sediments. Marine and Petroleum Geology 12, 195–204.

Robertson, E.C., 1983. Relationship of fault displacement to gouge and breccia thickness, 35. Society of Mining Engineers, American Institute of Mining Engineers Transactions, pp. 1426–1432.

Sample, J.C., Reid, M.R., Tobin, H.J., Moore, J.C., 1993. Carbonate cements indicate channeled fluid flow along a zone of vertical faults at the deformation front of the Cascadia accretionary wedge (northwest U.S. coast). Geology 21, 507–510.

Schneider, F., Wolf, S., Faille, I., Pot, D., 2000. A 3d basin model for hydrocarbon potential evaluation. Application to Congo offshore. Oil & Gas Science and Technology–Rev. IFP 55, 3–13.

Schowalter, T.T., 1979. Mechanics of secondary hydrocarbon migration and entrapment. AAPG Bulletin 63, 723–760.

Sibson, R.H., 1981. Fluid flow accompanying faulting: field evidence and models. In: Simpson, D.W., Richards, P.G. (Eds.), Earthquake Prediction: An International Review (Abs. 497). American Geophysical Union, Maurice Ewing Series 4, pp. 593–603.

Sibson, R.H., 1994. Crustal stress, faulting and fluid and fluid flow. In: Parnell, J. (Ed.), Geofluids. Origin, Migration and Evolution of Fluid in Sedimentary Basins, vol. 78. Geological Society Special Publication, London, pp. 69–84.

Sibson, R.H., Moore, J.M.M., Rankin, A.H., 1975. Seismic pumping – A hydrothermal fluid transport mechanism. Journal of Geological Society (London) 131, 653–659.

Skerlec, G.M., 1996. Risking fault seal in the Gulf Coast (abs.). AAPG Annual Convention Program and Abstracts 5, p. A131.

Smith, D.A., 1966. Theoretical consideration of sealing and nonsealing faults. AAPG Bulletin 50, 363–374.

Smith, D.A., 1980. Sealing and non-sealing faults in Louisiana Gulf Coast salt basin. AAPG Bulletin 64, 145–172.

Smith, L., Forster, C.B., Evans, J.P., 1990. Interaction of fault zones, fluid flow, and heat transfer at the basin scale. In: Neuman, S.P., Neretnieks, I. (Eds.), Hydrogeology of Low Permeability Environments, Hydrogeology Selected Papers 2, pp. 41–67.

Sorkhabi, R., Tsuji, Y., 2005. The place of faults in petroleum traps. In: Sorkhabi, R., Tsuji, Y. (Eds.), Faults, Fluid Flow, and Petroleum Traps. AAPG Memoir, vol. 85, pp. 1–31.

Sorkhabi, R., Hasegawa, S., Suzuki, K., Takahashi, M., Fujimoto, M., Sakuyama, N., Lwanaga, S., 2002. Modeling of shale smear parameters, fault seal potential, and fault rock permeability (abs.). AAPG Annual Meeting, 6.

Sperrevik, S., Gillespie, P.A., Fisher, Q.J., Halvorsen, T., Knipe, R.J., 2002. Empirical estimation of fault rock properties. In: Koestler, A.G., Hunsdale, R. (Eds.), Hydrocarbon Seal Quantification. Norwegian Petroleum Society (NPF), vol. 11. Special Publication, pp. 109–125.

Ungerer, P., Burrus, J., Doligez, B., Chenet, Y., Bessis, F., 1990. Basin evaluation by integrated two-dimensional modeling of heat transfer, fluid flow, hydrocarbon generation, and migration. AAPG Bulletin 74, 309–335.

Wang, G.Q., Qi, J.F., Yue, Y.F., 2003. Formation and evolution of the Cenozoic tectonics within and surrounding the Qikou Sag (in Chinese). Chinese Journal of Geology 38, 230–240.

Wang, G.Z., Yuan, S.Q., Xiao, L., 2006. Source conditions in Chengbei fault-step area and analysis on hydrocarbon migration (in Chinese). Journal of Oil and Gas Technology 28, 200–203.

Watts, N., 1987. Theoretical aspects of cap-rock and fault seals for single- and two-phase hydrocarbon columns. Marine and Petroleum Geology 4, 274–307.

Weber, K.J., Mandl, G., Pilaar, W.F., Lehner, F., Precious, R.G., 1978. The role of faults in hydrocarbon migration and trapping in Nigerian growth fault structures, 10. Offshore Technology Conference, pp. 2643–2653.

Xie, X.N., Li, S.T., Dong, W.L., Hu, Z.L., 2001. Evidence for episodic expulsion of hot fluids along faults near diapiric structures of the Yinggehai Basin, South China Sea. Marine and Petroleum Geology 18, 715–728.

Xu, Z.H., Wu, X., Qi, S.F., Zhang, D.N., 1996. Characteristics of contemporary tectonic stress in Beidagang oil Field and its vicinity (in Chinese). Petroleum Exploration and Development 23, 78–81.

Yielding, G., 2002. Shale gouge ratio calibration by geohistory. In: Koestler, A.G., Hunsdale, R. (Eds.), Hydrocarbon Seal Quantification. Norwegian Petroleum Society (NPF), vol. 11. Special Publication, pp. 1–15.

Yielding, G., Freeman, B., Needham, D.T., 1997. Quantitative fault seal prediction. AAPG Bulletin 81, 897–917.

Yu, C.H., Su, J.Q., Yuan, S.Q., Sheng, D.J., Duan, R.M., Zhang, L.K., 2006. Analysis of main control factors on oil and gas accumulation in Chengbei fault-step area, Dagang oil field (in Chinese). Sedimentary Geology and Tethyan Geology 26, 88–92.

Yuan, S.Q., Ding, X.L., Su, J.Q., Zhang, S.F., 2004. The research on forming conditions of reservoir in Chengbei step-fault zone, Dagang oil field (in Chinese). Journal of Jianghan Petroleum Institute 26, 8–9.

Zhang, L.K., Luo, X.R., Liao, Q.J., Yuan, S.Q., Xiao, D.Q., Wang, Z.M., Yu, C.H., 2007. Quantitative evaluation of fault sealing property with fault connectivity probabilistic method (in Chinese). Oil & Gas Geology 28, 181–191.

Zhang, L.K., Luo, X.R., Liao, Q.J., Yang, W., Guy, V., Yu, C.H., Su, J.Q., Yuan, S.Q., Xiao, D.Q., Wang, Z.M., 2010. Quantitative evaluation of synsedimentary fault opening and sealing properties using hydrocarbon connection probability assessment. AAPG Bulletin 94, 1379–1399.

Zhou, X.G., Sun, B.S., Tan, C.X., Tan, H.B., Zheng, R.Z., Ma, C.X., 2000. State of current geo-stress and effect of fault sealing (in Chinese). Petroleum Exploration & Development 27, 127–131.